Demonstration of 2:2 Stoichiometry in the Functional SRI−HtrI Signaling Complex in *Halobacterium* Membranes by Gene Fusion Analysis†

Xinpu Chen and John L. Spudich*

Department of Microbiology and Molecular Genetics, University of Texas Medical School at Houston, 6431 Fannin Street, Houston, Texas 77030

Received November 19, 2001; Revised Manuscript Received January 29, 2002

ABSTRACT: A fusion protein in which the C-terminus of *Halobacterium salinarum* sensory rhodopsin I (SRI) is connected by a flexible linker to the N-terminus of its transducer (HtrI) was constructed and expressed in *H. salinarum*. The fusion protein mediated attractant responses to orange light and repellent responses to UV/violet light that were comparable to those produced by the wild-type SRI−HtrI complex. Immunoblot analysis of *H. salinarum* membrane proteins demonstrated intact fusion protein and no detectable proteolytic cleavage products. Rapid oxidative cross-linking of a monocysteine mutant in the HtrI domain confirmed that the fusion protein exists as a homodimer in the membrane. HtrI-free SRI and HtrI-complexed SRI have been shown previously to exhibit large differences in the pH dependence of their photocycle kinetics and in the pK_a of Asp76 that controls a pH-dependent spectral transition in SRI. These differences were used to assess whether only one or both SRI domains in the fusion protein were complexed properly to the HtrI homodimer. Measurement of the photochemical activity, the photocycle kinetics, and the absorption spectra at various pH values established that both SRI domains are complexed to HtrI in the fusion protein, and therefore the stoichiometry is 2:2. Closer examination of the HtrI effect on SRI revealed that Asp76 titration in HtrI-free SRI fits two pK_a values, with 98% and 2% of the molecules titrating with pK_a's of 7 and 9, respectively. The same two pK_a's of Asp76 are evident in HtrI-complexed SRI, but with 13% with pK_a of 7 and 87% with pK_a of 9 and a similar bias toward the pK_a of 9 in the fusion protein. Titration of the fusion protein with Ala substitution at Arg73, a residue in the photoactive site, in the SRI domain indicates that a basic residue at Arg73 is necessary for the lower pK_a to be observed. A model in which Arg73 plays a role in the HtrI effect on SRI is discussed.

Sensory rhodopsin I (SRI,[1] λ_{max} 587) is a phototaxis receptor which is complexed with its membrane-embedded transducer (HtrI) to mediate attractant responses to orange light and repellent responses to UV/violet light (*1*, *2*). Photon absorption by the dark form of SRI, SR_{587}, leads to the transient deprotonation of its retinylidene Schiff base (*3*) and the formation of its attractant signaling state, S_{373} (λ_{max} 373) (*4*). A second photon absorbed by S_{373} regenerates SR_{587} and causes a repellent response (*5*). In the absence of UV/violet light, S_{373} returns thermally within seconds to the SR_{587} state. The kinetics of S_{373} thermal decay is greatly influenced by its complexation to its cognate transducer HtrI (*6*−*8*). S_{373} decay is pH-independent with a half-life of ∼800 ms for HtrI-complexed SRI, while S_{373} decay is pH-dependent in HtrI-free SRI, with a half-life varying from ∼80 ms at pH 4 to ∼4 s at pH 7 at 23 °C. Therefore, flash-induced absorption measurements of S_{373} decay in the SRI photocycle provide a useful assay for SRI−HtrI interaction.

A second assay for SRI−HtrI interaction is provided by the HtrI influence on a shift in its absorption spectrum, the "blue-purple transition", undergone by SRI as the pH is increased (*9*−*11*). The alkaline-induced shift in its absorption maximum is from 587 nm (blue form) to 552 nm (purple form) and is due to the deprotonation of Asp76, a counterion to the protonated Schiff base in the receptor. HtrI interaction with SRI raises the pK_a of Asp76, thereby altering the pH at which the blue-purple transition occurs. In the SRI−HtrI complex, the transition occurs with a pK_a of ∼9, whereas it occurs with a pK_a of ∼7 in the absence of HtrI.

HtrI appears to form a homodimer in the *Halobacterium salinarum* membrane (*12*) as do the eubacterial taxis transducers, such as the *Salmonella typhimurium* and *Escherichia coli* aspartate chemotaxis receptor Tar (*13*−*17*). Each Tar dimer binds one maltose binding protein (MBP) as an attractant ligand, and therefore at saturation the molar ratio [MBP]:[Tar] is 1:2 (*18*). The attractant ligand aspartate also exhibits half-of-the-sites binding to the Tar dimer (*19*). It is not clear whether 1 or 2 SRI molecules associate with the HtrI dimer in the membrane. As with any symmetrical homodimer, two identical binding sites must exist, but one

† This work was supported by National Institutes of Health Grant R01GM27750.

* Corresponding author. Telephone: 713-500-5458. Fax: 713-500-5499. E-mail: John.L.Spudich@uth.tmc.edu.

[1] Abbreviations: SRI, sensory rhodopsin I from *Halobacterium salinarum*; HtrI, the transducer associated with SRI; TM1 and TM2, the N-terminal proximal and distal transmembrane segments of HtrI; NpSRII and NpHtrII, *Natronobacterium pharaonis* SRII and HtrII, respectively; SR_{587} and SR_{552}, the blue acidic and purple alkaline forms of unphotolyzed SRI; S_{373}, the deprotonated Schiff base intermediate in the SRI photocycle; *bop*, gene encoding bacteriorhodopsin (BR) apoprotein; *sopI*, gene encoding SRI apoprotein; HR, halorhodopsin. Mutant forms of SRI and HtrI are designated with the single-letter code; for example, SRI-R73A indicates substitution of the residue at position 73 in SRI with an alanine residue; HtrI-G29C indicates substitution of the residue at position 29 in HtrI with a cysteine residue.

10.1021/bi015966h CCC: $22.00
Published on Web 02/27/2002

may be occluded by occupancy of the other, as occurs with MBP binding to Tar. We undertook to answer this question by forcing equal membrane molar content of SRI to HtrI by expressing a fusion of the *sopI* and *htrI* genes in a strain lacking both proteins. If the ratio in the membrane complex were 1:2, we would observe 50% complexed and 50% free SRI, whereas if both binding sites on the HtrI dimer could be simultaneously occupied, we would observe 100% complexed SRI. These two possibilities are readily distinguished by absorption and kinetic spectroscopy.

MATERIALS AND METHODS

Plasmids and Strains. Wild-type SRI−HtrI complexes were expressed from their native promoter in plasmid pKJ306 (*4*), and HtrI-free SRI was expressed under the *bop* promoter in plasmid pTR2 (*7*). Pho81Wr$^-$ (BR$^-$HR$^-$SRI$^-$HtrI$^-$ SRII$^-$HtrII$^-$, carotenoid deficient and restriction deficient) (*20*) was used as the *H. salinarum* recipient in plasmid transformations.

Construction of the Plasmid Encoding the SRI−HtrI Fusion Protein. A 720 bp *Nsi*I/*Nco*I *sopI* gene fragment (PCR product from plasmid pKJ306), a 2.2 kb *Not*I/*Nco*I *bop* promoter region, and a 4.4 kb *Not*I/*Nsi*I fragment of plasmid pKJ410 were ligated together to form plasmid pXP2, where the *sopI* gene is under the control of the *bop* promoter. The pKJ410 is a pKJ306 derivative which contains the HtrI gene under the *bop* promoter. An 890 bp *Sac*I/*Xba*I fragment (a PCR product from plasmid pKJ306) encoding the C-terminus of HtrI replaced a 1.3 kb *Sac*I/*Xba*I fragment of plasmid pKJ410 to form plasmid pXP3. Recombinant PCR was used to introduce 27 nucleotides (5′-GCGTCGGCGTC-GAACGGCGCGTCGGCG-3′) encoding a 9-residue flexible linker (Ala-Ser-Ala-Ser-Asn-Gly-Ala-Ser-Ala) (*21*) between the C-terminal residue of SRI and N-terminal residue of HtrI. This 1.9 kb *Bam*HI/*Sac*I recombinant fragment starting from the *Bam*HI site of the bop promoter and ending at the *Sac*I site of HtrI replaced a 1.1 kb *Sac*I/*Bam*HI fragment of plasmid pXP3 to form plasmid pXP6, where the SRI−HtrI fusion is under the control of the *bop* promoter. All the mutations were introduced by the two-step megaprimer PCR method with pfu polymerase (*22*).

Motion Analysis. Motility responses to SRI photoactivation were assayed by computer-assisted cell tracking and motion analysis as described (*4*). Swimming cells were subjected to a 4 s step-down in 600 nm light to test attractant signaling and a 150 ms step-up in 400 nm light in an orange background to test repellent signaling.

Membrane Preparation. Membranes were prepared by sonication of cells grown as described (*23*) to stationary phase in complex medium containing 1 μg/mL mevinolin. Membranes were suspended in 4 M NaCl/25 mM Tris-HCl (pH 6.8) at ∼10 mg of protein/mL in the final step of the procedure.

Flash Photolysis. Flash-induced absorption changes were measured by a laboratory-constructed cross-beam spectrometer with a frequency-double Nd:YAG laser (532 nm, 6 ns pulse, 40 mJ) providing the actinic flash (*24*). The flashing frequency was 0.08 Hz. A total of 16−32 transients were averaged for each trace at a constant temperature of 18 °C. The relative flash yields of SRI photocycling were calculated as $\Delta A_{590}/A_{587}$, where ΔA_{590} is the maximum amplitude of absorption change at 590 nm following the flash and A_{587} is the SRI absorbance at 587 nm, determined by difference spectroscopy using retinal regeneration of NH_2OH-bleached membranes (*25*).

pH Titration. The pH of the pigment suspension was measured with a Beckman Φ72 pH meter after sodium hydroxide solution was added in microliter quantities to the cuvette. Absorption difference spectra were recorded with an SLM-Aminco UV−vis spectrophotometer (SLM-Aminco, Urbana, IL). The change in absorption of the suspension at 600 nm, the wavelength of largest change in the blue minus purple SRI difference spectrum, was used as a quantitative measure of the blue-purple transition from spectra adjusted for baseline drift by fixing the value at 750 nm, at which neither the blue nor purple SRI absorbs. Care was taken to accept only data sets in which the isosbestic point for the blue-purple transition was maintained throughout the titration. All samples were in 4 M NaCl. Fits to the titration data were performed with algorithms from SigmaPlot (Jandel, San Rafael, CA).

Disulfide Cross-Linking Analysis. Oxidative cross-linking of engineered cysteine residues was carried out as described previously using Cu(II)-(1,10-phenanthroline)$_3$ as a catalyst (*12*). Treated samples were incubated at room temperature for 30 min and separated by SDS−PAGE in nonreducing conditions and immunoblotted with anti-SRI antibody.

RESULTS AND DISCUSSION

Expression of the Fusion Protein. The 130 kDa fusion protein consisting of SRI connected to HtrI via a 9-residue flexible linker (*21*) was expressed in *H. salinarum*; membrane proteins were separated by SDS−polyacrylamide gel electrophoresis and analyzed by immunoblot with anti-HtrI antibody and anti-SRI antibody. The fusion protein migrates as single bands on both immunoblots (Figure 1) with no detectable bands at the HtrI position nor at the SRI position on the respective immunoblots. We conclude that the fusion protein is intact in the *H. salinarum* membrane.

Phototaxis Responses. Pho81Wr$^-$ cells containing the wild-type SRI−HtrI complex exhibit attractant responses to orange light assessed by the induction of swimming reversals by a step-down of 600 nm light intensity and repellent responses to UV/violet light assessed by the induction of swimming reversals by a step-up of 400 nm light in an orange background. Pho81Wr$^-$ cells containing the fusion construct exhibited similar attractant responses to orange light and repellent responses to UV/violet light (Figure 2), indicating that the 9-residue linker does not inhibit functional interaction between the receptor and the transducer in vivo.

Dimer Formation between the HtrI Portions of the Fusion Protein. Some monocysteine mutants of wild-type HtrI form cross-linked dimers upon oxidative disulfide formation, indicating that HtrI, like eubacterial chemotaxis transducers, assembles into homodimers (*12*). To test the fusion protein for dimerization, we introduced a cysteine into the first transmembrane helix (TM1) of the HtrI portion [at position 29 in HtrI numbering (*26*)], corresponding to a position in a related Htr protein, NpHtrII, that exhibits rapid disulfide cross-linking (*27*). Membrane proteins were separated on nonreducing SDS−polyacrylamide gels and immunoblotted with anti-SRI antibody. Most of the monocysteine fusion

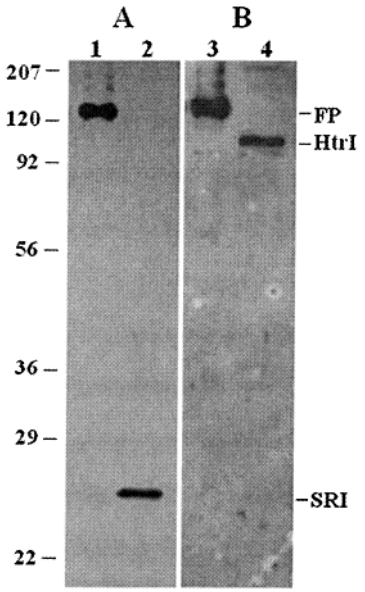

FIGURE 1: Immunoblot analysis of membranes containing the wild-type SRI−HtrI complex and fusion protein (FP). Membrane suspensions of the wild-type complex (lanes 2 and 4) and fusion protein (lanes 1 and 3) constructs were electrophoresed on a 10% SDS−polyacrylamide gel, transferred to poly(vinylidene difluoride) (PVDF) membranes, and probed with anti-SRI (A) and anti-HtrI (B) antibody. The positions of fusion protein (FP), HtrI, and SRI are indicated to the right.

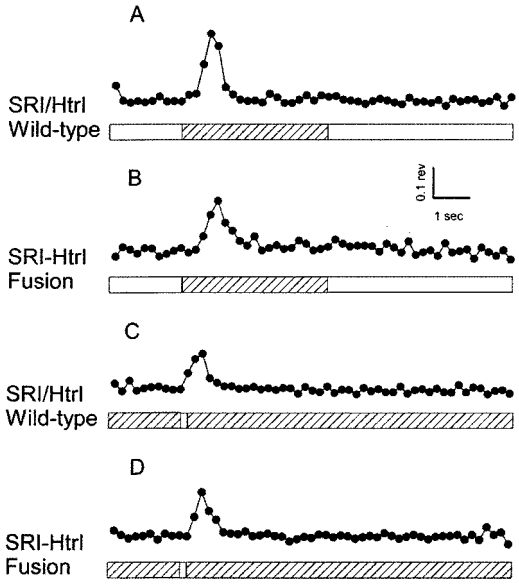

FIGURE 2: Phototaxis responses. Cells containing the wild-type SRI−HtrI complex and cells containing fusion protein were subjected to a 4 s step-down of orange light (A, B) and a 150 ms step-up of 400 nm light in an orange light background (C, D) 2 s after initiation of data acquisition. Traces represent population reversal frequency transients collected by computerized motion analysis at pH 6.0 and 40 °C. The bar on the vertical axis indicates 0.1 reversal per 200 ms frame.

protein was dimerized before catalyst was added, and the remainder formed a cross-linked dimer within 30 s at room temperature (Figure 3). The rapid and complete cross-linking of the monocysteine-substituted fusion protein indicates that the SRI portion and the 9-residue linker do not disrupt dimer formation of the HtrI part of the fusion protein.

The Flash Yield and Photocycle Kinetics of the Fusion Protein in H. salinarum Membrane Match Those of the HtrI-Complexed SRI. The photochemical reaction of SRI consists of flash-induced conversion of SR_{587} to S_{373} and a first-order thermal return of S_{373} to SR_{587}. These processes result in a transient depletion of absorption at 590 nm and a transient increase of absorption at 400 nm following a laser flash (532 nm, 6 ns). There are two readily monitored differences in the photochemical behavior between HtrI-complexed SRI and HtrI-free SRI. First, in the absence of HtrI, the flash yield of the S_{373} intermediate in free SRI is only 15−20% that of HtrI-complexed SRI (*6*). To measure flash yields, we subjected the membranes to NH_2OH bleaching (*25*), monitored SRI generation by reconstitution of the membranes with *all-trans*-retinal to quantitate the extinction of unphotolyzed SRI at 590 nm, and examined these membranes with known SRI content by laser flash photolysis. The flash yields at 590 nm, measuring SR_{587} depletion and return, and at 400 nm, measuring S_{373} formation, of free SRI were 20% and 18%, respectively, of the yields in the wild-type SRI−HtrI complex (Table 1), confirming the previous report. The yields of the fusion protein were nearly identical to those of the wild-type complex. If 50% of the SRI in the fusion protein were free, as would occur if the stoichiometry were one receptor per transducer dimer, then the fusion protein yield would be expected to be the average of the free SRI and wild-type complex values. By this criterion there is undetectable free SRI in the fusion protein-containing membranes.

A second difference between free and HtrI-complexed SRI is the pH dependence of the S_{373} decay rate (*6*, *7*). In the absence of HtrI, S_{373} decay is strongly pH-dependent, increasing from ∼80 ms at pH 4 to ∼4 s at pH 7, whereas the $t_{1/2}$ of S_{373} decay of HtrI-complexed SRI exhibits a nearly constant decay $t_{1/2}$ of ∼800 ms in this pH range. This influence of HtrI has a dramatic effect on SR_{587} depletion and return, rendering the photocycle of free SRI markedly slower than that of the complexed form at higher pH 6.8 and markedly faster at lower pH 5.0 (Figure 4). In contrast, the flash-induced transient absorbance changes of fusion protein are pH-independent and are indistinguishable from those of the wild-type complex at both the lower and higher

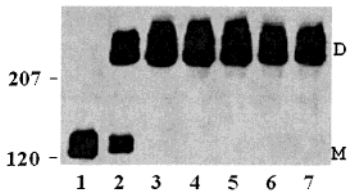

FIGURE 3: Oxidative cross-linking of single cysteine-substituted HtrI-G29C of the fusion protein. Oxidative cross-linking catalyzed by Cu(II)-(1,10-phenanthroline)$_3$ was performed with the membrane suspension at room temperature at various times after catalyst addition. A membrane suspension containing wild-type fusion protein (without cysteine) was used to indicate the position of the monomer. Lanes: 1, wild-type fusion protein; 2−7, 0, 0.5, 1, 2, 3, and 15 min cross-linking reaction of single cysteine-substituted HtrI-G29C of the fusion protein. Abbreviations: M, monomer; D, dimer.

Table 1: Photochemical Reaction Flash Yield (%) of *H. salinarum* Membranes at pH 6.0

	monitored wavelength	
	590 nm	400 nm
HtrI-free SRI	2.8	1.5
wild-type SRI−HtrI complex	13.8	8.2
fusion protein	14.2	8.7

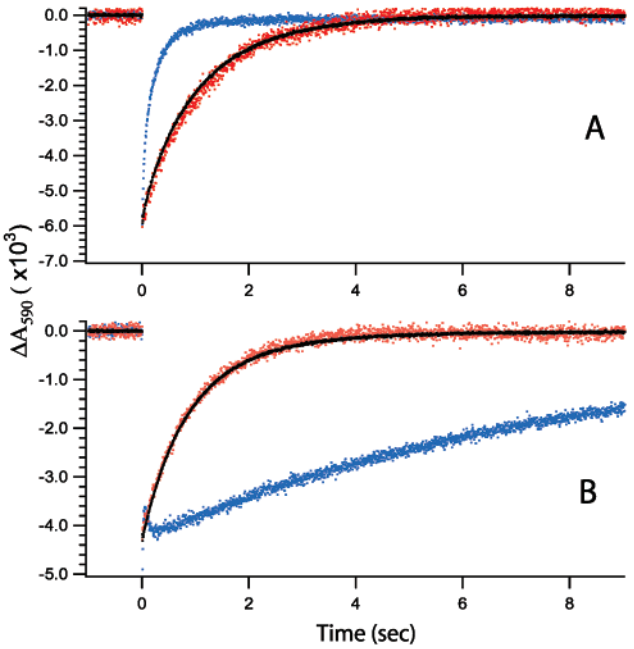

FIGURE 4: Flash-induced absorption transients at 590 nm of HtrI-free SRI, HtrI-complexed SRI, and the fusion protein. The membrane suspension containing HtrI-free SRI (blue trace), HtrI-complexed SRI (red trace), and the fusion protein (black trace) was subjected to a 532 nm laser (6 ns), and absorption transients were monitored at 590 nm. (A) pH 5.0; (B) pH 6.8. The three traces in each panel were scaled to the same amplitude for comparison. The amplitudes on the vertical axes are those for HtrI-free SRI. Maximum depletion amplitudes for the other traces were as follows: (A) HtrI-complexed SRI, 3.0×10^{-3} absorption unit; fusion protein, 2.0×10^{-2}; (B) HtrI-complexed SRI, 3.6×10^{-3}; fusion protein, 2.2×10^{-2}. Note that the relatively large signals of the fusion protein (black trace) result in a narrow noise envelope, which should not be mistaken for a fitted curve.

pH values (Figure 4). We conclude that also based on this criterion both SRI molecules in the fusion protein dimer are complexed with HtrI.

pH Titration of the Blue-Purple Transition. SRI exhibits a shift in its absorption maximum from 587 to 552 nm at alkaline pH, which has been referred to as the blue-purple transition (*1*). This transition is caused by the deprotonation of Asp76, which blue shifts the absorption maximum of SRI by contributing counterion stabilization of the protonated Schiff base in the 552 nm (purple) species (*11*). In the blue species, SR_{587}, Asp76 is protonated. The pK_a of Asp76, and therefore of the blue-purple transition, is shifted 2 pH units by HtrI interaction from ~7 to ~9 (*10*, *28*, *29*). This difference provides a third test of the state of SRI in the fusion protein.

The pH titrations of the blue-purple transition for SRI in membranes containing HtrI-free SRI, wild-type HtrI-complexed SRI, and the fusion protein are shown in Figure 5. When fitted to a monoprotic titration, the HtrI-free SRI and wild-type HtrI-complexed SRI exhibit pK_a values of 7.4 and 8.7, confirming the previous reports (*10*, *28*, *29*). The titration of the fusion protein closely matches that of wild-type HtrI-complexed SRI and not that of the theoretical titration curve that would result if the fusion protein contained 50% free and 50% complexed SRI (Figure 5A).

The above results establish that both SRI binding sites in the HtrI homodimer are capable of simultaneously binding to SRI when the molecules are folded into a functional

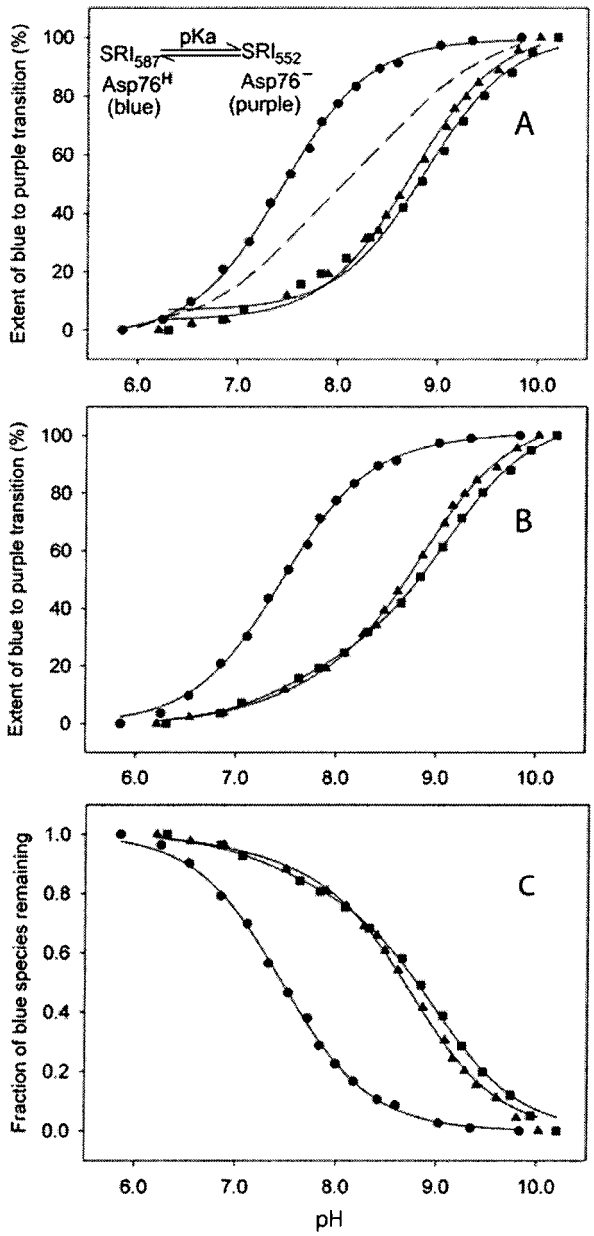

FIGURE 5: pH titration of HtrI-free SRI, HtrI-complexed SRI, and the fusion protein. Sodium hydroxide solution was added incrementally to the membrane suspension containing HtrI-free SRI, HtrI-complexed SRI, and the fusion protein, and the pH and absorption difference spectrum were measured after each addition. (A) The decrease of absorption at 600 nm was plotted as the percentage of the blue (λ_{max} 587 nm) to purple (λ_{max} 552 nm) transition against pH. pH titration data were fit to a single pK_a. The single pK_a values for HtrI-free SRI (●), HtrI-complexed SRI (▲), and the fusion protein (■) from the fits are 7.4, 8.7, and 8.9 respectively. (- - -) indicates the theoretical titration curve of the sample containing 50% HtrI-free SRI and 50% HtrI-complexed SRI. (B) The same pH titration data were fit to two uncoupled pK_a values. The two pK_a values fit for HtrI-free SRI (●) produced pK_a 7.4, 97.9%, and pK_a 9.3, 2.1%. The two pK_a values fit for HtrI-complexed SRI (▲) gave pK_a 7.4, 12.7%, and pK_a 8.9, 87.3%. The two pK_a values fit for the fusion protein (■) gave pK_a 7.5, 21.8%, and pK_a 9.1, 78.2%. (C) Fractions of untitrated Asp76 of HtrI-free SRI, HtrI-complexed SRI, and the fusion protein were calculated from the same pH titration data. The fits were obtained by using the Balashov−Ebrey model (for equation, see text). The fit for free SRI (●) gave pK_{a1} 7.5, pK_{a2} 8.9, pK_{a3} 8.8, and pK_{a4} 7.6. The fit for HtrI-complexed SRI (▲) gave pK_{a1} 8.1, pK_{a2} 7.7, pK_{a3} 7.1, and pK_{a4} 8.7. The fit for the fusion protein (■) gave pK_{a1} 8.1, pK_{a2} 8.3, pK_{a3} 7.5, and pK_{a4} 8.9.

complex in the *H. salinarum* membrane and that the HtrI dimer modulates the properties of both SRI molecules in the same manner as in the wild-type SRI−HtrI complex. SRI molecules in the fusion protein behave as HtrI-complexed receptors rather than as free SRI based on measurements of photoreaction yield, pH effects on the photocycle kinetics, and the pH titration of the blue-purple transition, each of which is diagnostic of the complexed versus free state of SRI. Our results obtained with the full-length SRI−HtrI proteins in the native cell membrane are consistent with in vitro measurements with purified components that indicate equal molar content of NpSRII and an N-terminal fragment of NpHtrII in molecular complexes (*30*, *31*).

The capability of forming 2:2 complexes is not inconsistent with a lower molar ratio of SRI to HtrI in the wild-type cell. From the same types of measurements made here, free SRI is undetectable in wild-type membranes (*7*). HtrI may be in excess of SRI in wild-type cells and therefore not be saturated with SRI, in which case both 1:2 and 2:2 signaling complexes may occur, or at low SRI:HtrI molar ratios essentially only 1:2 complexes might exist. In this regard, measurements of absolute concentrations (*32*) and rotational diffusion measurements (*33*) of SRI in wild-type membranes have suggested ratios closer to 1:2 than 2:2. We emphasize that our results show that SRI and HtrI form 2:2 active complexes and that SRI is properly coupled to HtrI according to spectroscopic criteria, but our results do not distinguish whether one or two independent signals could be generated through such complexes.

Models To Fit the Titration Behavior of HtrI-Free SRI, HtrI-Complexed SRI, and Fusion Protein. The single pK_a fits to the three sets of titration data produced different pK_a values, 7.4 in the case of HtrI-free SRI and 8.7 and 8.9, respectively, for the wild-type complex and the fusion protein. These fits readily distinguish free from complexed behavior of SRI, but the single pK_a fit to the titration data exhibits significant deviation from the data for the HtrI-complexed SRI and for the fusion protein (Figure 5A). Accordingly, we examined fitting the three data sets with alternative models.

A simple two pK_a model for the titration data fits all three titration data sets very well (Figure 5B). Independent fits to each of the three data sets produce essentially the same two pK_a values (7.4−7.5 and 8.9−9.3) with different relative amplitudes, indicating consistent behavior of this model. A physical interpretation of these results would be that there are two distinct forms of SRI, one in which Asp76 exhibits a pK_a of 7 and the other in which the Asp76 pK_a is 9, and the latter species is stabilized by HtrI interaction.

The pH titration of the blue-purple transition of SRI is governed by the titration of residue Asp76 (*1*). In bacteriorhodopsin (BR), a similar blue-purple transition results from titration of the residue Asp85, which corresponds in position to Asp76 in SRI (*11*, *34*−*36*). A second model to explain the complex titration behavior of SRI is based on previous analysis of BR. Careful titration over a wide range of values established that titration of Asp85 in BR exhibits deviation from a simple monoprotic titration equation (*37*, *38*). To explain their data, the authors proposed that the pK_a of Asp85 is coupled to that of another titratable residue X in BR. In the Balashov−Ebrey model, the pH dependence of the fraction of protonated Asp85 is a function of three independent parameters (*38*): $f_{DH}(pH) = \alpha/(\alpha + \beta\gamma)$, where $\alpha = 1 + 10^{pH-pK_{a3}}$, $\beta = 1 + 10^{pH-pK_{a2}}$, and $\gamma = 10^{pH-pK_{a1}}$; pK_{a2} and pK_{a3} are the pK_a's of X when Asp85 is deprotonated or protonated, respectively, and pK_{a1} is the pK_a of Asp85 when X is protonated. pK_{a4}, the pK_a of Asp85 when X is deprotonated, is defined by the relation $pK_{a4} = pK_{a1} + pK_{a2} - pK_{a3}$. Studies of mutants of BR indicate that X is not a single residue but rather is a complex of residues including Arg82 (*39*), which forms a quadrupole ion complex with the protonated Schiff base, Asp85, and Asp212 (*40*−*42*).

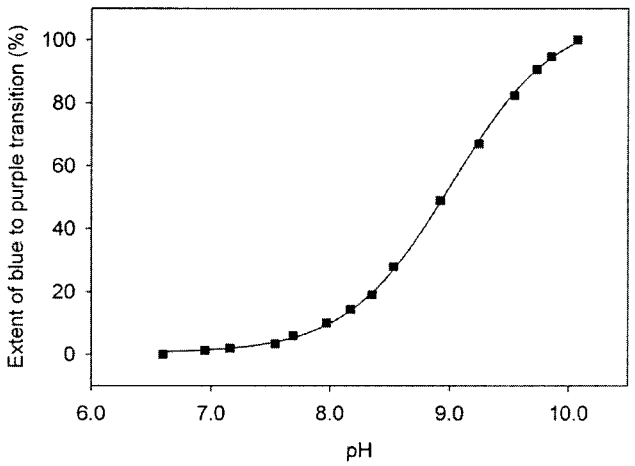

FIGURE 6: pH titration of the R73A fusion protein. Titration data of the R73A fusion protein were fit to a single pK_a of 9.0.

We applied the Balashov−Ebrey model to our data and obtained fits to the three data sets (Figure 5C) approximately as good as that of the simple two pK_a model (Figure 5B). For HtrI-free SRI the fit converges to a condition in which the Asp76 and X protonation states have very little influence on the pK_a values of the other group; i.e., the coupling strength is small (0.1) and therefore the pK_{a1} and pK_{a2} values are close to pK_{a4} and pK_{a3}, respectively. For the wild-type HtrI-complexed SRI and the fusion protein, the data fit with the Asp76 pK_a shifting from 8.1 to 8.7−8.9 upon deprotonation of X. This occurs in the same direction as in BR, in which X deprotonation shifts the Asp85 pK_a from 2.6 to 7.5 but is a more moderate effect in SRI. In terms of this model, the effect of HtrI on the pK_a of Asp76 can be dissected into two separate effects. First, the pK_a of Asp76 is raised from 7.5 to 8.1 by structural changes induced by transducer interaction, and second, HtrI increases coupling of the pK_a of the titratable group X to that of Asp76, further increasing the apparent pK_a of the blue-purple transition.

By analogy with the suggested role of Arg82 in BR as part of X in the Balashov−Ebrey model (*38*), one of the coupled residues in SRI may be Arg73. To test this notion, we constructed plasmids encoding R73A mutants of HtrI-free SRI and of the fusion protein. No visible pigment was produced in the R73A HtrI-free SRI mutant; however, pigment was produced in the corresponding R73A fusion protein. The titration data of the R73A fusion protein fit a single pK_a of 9.0 (Figure 6), consistent with Arg73/Asp76 pK_a coupling being responsible for the complex titration behavior. The result is also consistent with the alternative interpretation that there are two distinct forms of SRI, one in which Asp76 exhibits a pK_a of 7 and the other in which the Asp76 pK_a is 9, and the lower pK_a species requires a positive charge on the residue at position 73 in SRI.

ACKNOWLEDGMENT

We thank Elena Spudich, Kwang-Hwan Jung, Vishwa Trivedi, Chii-Shen Yang, and Weiwu Wang for critical reading and comments on the manuscript.

REFERENCES

1. Hoff, W. D., Jung, K. H., and Spudich, J. L. (1997) *Annu. Rev. Biophys. Biomol. Struct. 26*, 223−258.
2. Oesterhelt, D. (1998) *Curr. Opin. Struct. Biol. 8*, 489−500.
3. Haupts, U., Eisfeld, W., Stockburger, M., and Oesterhelt, D. (1994) *FEBS Lett. 356*, 25−29.
4. Jung, K. H., and Spudich, J. L. (1998) *J. Bacteriol. 180*, 2033−2042.
5. Spudich, J. L., and Bogomolni, R. A. (1984) *Nature 312*, 509−513.
6. Spudich, E. N., and Spudich, J. L. (1993) *J. Biol. Chem. 268*, 16095−16097.
7. Olson, K. D., and Spudich, J. L. (1993) *Biophys. J. 65*, 2578−2585.
8. Szundi, I., Swartz, T. E., and Bogomolni, R. A. (2001) *Biophys. J. 80*, 469−479.
9. Bogomolni, R. A., Stoeckenius, W., Szundi, I., Perozo, E., Olson, K. D., and Spudich, J. L. (1994) *Proc. Natl. Acad. Sci. U.S.A. 91*, 10188−10192.
10. Olson, K. D., Zhang, X. N., and Spudich, J. L. (1995) *Proc. Natl. Acad. Sci. U.S.A. 92*, 3185−3189.
11. Rath, P., Spudich, E., Neal, D. D., Spudich, J. L., and Rothschild, K. J. (1996) *Biochemistry 35*, 6690−6696.
12. Zhang, X. N., and Spudich, J. L. (1998) *J. Biol. Chem. 273*, 19722−19728.
13. Milligan, D. L., and Koshland, D. E., Jr. (1988) *J. Biol. Chem. 263*, 6268−6275.
14. Milburn, M. V., Prive, G. G., Milligan, D. L., Scott, W. G., Yeh, J., Jancarik, J., Koshland, D. E., Jr., and Kim, S. H. (1991) *Science 254*, 1342−1347.
15. Pakula, A. A., and Simon, M. I. (1992) *Proc. Natl. Acad. Sci. U.S.A. 89*, 4144−4148.
16. Chervitz, S. A., and Falke, J. J. (1995) *J. Biol. Chem. 270*, 24043−24053.
17. Kim, K. K., Yokota, H., and Kim, S. H. (1999) *Nature 400*, 787−792.
18. Gardina, P. J., Bormans, A. F., Hawkins, M. A., Meeker, J. W., and Manson, M. D. (1997) *Mol. Microbiol. 23*, 1181−1191.
19. Biemann, H. P., and Koshland, D. E., Jr. (1994) *Biochemistry 33*, 629−634.
20. Yao, V. J., Spudich, E. N., and Spudich, J. L. (1994) *J. Bacteriol. 176*, 6931−6935.
21. Jones, P. C., and Fillingame, R. H. (1998) *J. Biol. Chem. 273*, 29701−29705.
22. Chen, B., and Przybyla, A. E. (1994) *BioTechniques 17*, 657−659.
23. Bogomolni, R. A., and Spudich, J. L. (1995) in *Archaea: a laboratory manual* (Robb, F. T., Place, A. R., Sowers, K. R., Schreier, H. J., DasSarma, S., and Fleischmann, E. M., Eds.) pp 63−73, Cold Spring Harbor Laboratory Press, Plainview, NY.
24. Sasaki, J., and Spudich, J. L. (1998) *Biophys. J. 75*, 2435−2440.
25. Spudich, E. N., Sundberg, S. A., Manor, D., and Spudich, J. L. (1986) *Proteins 1*, 239−246.
26. Yao, V. J., and Spudich, J. L. (1992) *Proc. Natl. Acad. Sci. U.S.A. 89*, 11915−11919.
27. Yang, C. S., and Spudich, J. L. (2001) *Biochemistry 40*, 14207−14214.
28. Spudich, J. L. (1994) *Cell 79*, 747−750.
29. Haupts, U., Haupts, C., and Oesterhelt, D. (1995) *Proc. Natl. Acad. Sci. U.S.A. 92*, 3834−3838.
30. Sudo, Y., Iwamoto, M., Shimono, K., and Kamo, N. (2001) *Photochem. Photobiol. 74*, 489−494.
31. Wegener, A. A., Klare, J. P., Engelhard, M., and Steinhoff, H. J. (2001) *EMBO J. 20*, 5312−5319.
32. Perazzona, B. (1999) Role of transducer proteins in phototaxis signaling of *Halobacterium salinarum*, Ph.D. Dissertion, Graduate School of Biomedical Sciences, The University of Texas Health Science Center at Houston, Houston, TX.
33. Bogomolni, R. A., Fukushima, J. G, Swartz, T., and Szundi I. (1997) *Biophys. J. 72*, A16.
34. Subramaniam, S., Marti, T., and Khorana, H. G. (1990) *Proc. Natl. Acad. Sci. U.S.A. 87*, 1013−1017.
35. Metz, G., Siebert, F., and Engelhard, M. (1992) *FEBS Lett. 303*, 237−241.
36. Rath, P., Olson, K. D., Spudich, J. L., and Rothschild, K. J. (1994) *Biochemistry 33*, 5600−5606.
37. Balashov, S. P., Govindjee, R., Imasheva, E. S., Misra, S., Ebrey, T. G., Feng, Y., Crouch, R. K., and Menick, D. R. (1995) *Biochemistry 34*, 8820−8834.
38. Balashov, S. P., Imasheva, E. S., Govindjee, R., and Ebrey, T. G. (1996) *Biophys. J. 70*, 473−481.
39. Balashov, S. P. (2000) *Biochim. Biophys. Acta 1460*, 75−94.
40. Der, A., Szaraz, S., Toth-Boconadi, R., Tokaji, Z., Keszthelyi, L., and Stoeckenius, W. (1991) *Proc. Natl. Acad. Sci. U.S.A. 88*, 4751−4755.
41. Marti, T., Rosselet, S. J., Otto, H., Heyn, M. P., and Khorana, H. G. (1991) *J. Biol. Chem. 266*, 18674−18683.
42. Marti, T., Otto, H., Rosselet, S. J., Heyn, M. P., and Khorana, H. G. (1992) *J. Biol. Chem. 267*, 16922−16927.

BI015966H